Available online at www.sciencedirect.com

SCIENCE DIRECT®

Earth and Planetary Science Letters 236 (2005) 751–764

EPSL

www.elsevier.com/locate/epsl

High-precision constraints on timing of Alpine warm periods during the middle to late Pleistocene using speleothem growth periods

Steffen Holzkämper [a,*], Christoph Spötl [b], Augusto Mangini [a]

[a] *Forschungsstelle Radiometrie, Heidelberger Akademie der Wissenchaften, Im Neuenheimer Feld 229, 69120 Heidelberg, Germany*
[b] *Institut für Geologie und Paläontologie, Leopold-Franzens-Universität Innsbruck, Innrain 52, 6020 Innsbruck, Austria*

Received 14 December 2004; received in revised form 6 April 2005; accepted 1 June 2005
Available online 11 July 2005
Editor: B. Wood

Abstract

A long-standing problem in the reconstruction of warm climate periods during the late Quaternary is the difficulty of determining absolute ages for undisturbed terrestrial climate archives. Speleothems offer an important source of information about the timing and duration of middle and late Pleistocene warm phases. A flowstone from the high-elevation Spannagel Cave (Zillertal Alps, Austria) provides a new absolutely dated climate record, which includes the most prominent warm phases between ~260 and 50 ka before present. New data from the Penultimate Interglacial improve our knowledge about the timing and progression of warm periods in the Alps corresponding to marine isotope stages 7 and 8. Speleothem growth phases were identified from ~261 to 249, from ~236 to 229, and from ~200 to 192 ka. An early onset of the Last Interglacial is corroborated by a growth phase commencing at 136.7 ± 2.8 ka and the youngest section of the flowstone provides further evidence for an Alpine climate during time intervals corresponding to marine isotope stages 5a and 3 sufficiently warm to allow speleothems to grow. The high-resolution stable isotope profile taken along the growth axis of the flowstone provides information about the hydrological conditions during the growth phases.

Keywords: speleothems; stable isotopes; high alpine climate; Penultimate Interglacial; Last Interglacial

1. Introduction

The past 260 ka were dominated by large fluctuations in global climate [1,2]. Major warm phases accompanied by sea level high stands have been identified in stacked $\delta^{18}O$ records from five widely distributed marine sediment cores (SPECMAP) and

* Corresponding author. Present address: Department of Physical Geography and Quaternary Geology, Stockholm University, 106 91 Stockholm, Sweden. Tel.: +46 8 16 4891; fax: +46 8 16 4818.
E-mail address: steffen.holzkaemper@natgeo.su.se (S. Holzkämper).

0012-821X/$ - see front matter © 2005 Elsevier B.V. All rights reserved.
doi:10.1016/j.epsl.2005.06.002

according to the time scale of [3] they span the periods from 245 to 186 ka (marine isotope stage 7 (MIS 7)), 128 to 71 ka (MIS 5), 59 to 24 ka (MIS 3), and from 12 ka to the present (MIS 1). Slightly different dates for the stage boundaries are given in [4], where a different tuning technique was used and which is based on one high-resolution sediment core from the south-western sub-polar Indian Ocean. The time scale of these warm stages is mainly based on the Earth's orbital parameters and a universally accepted absolute time scale for the last three glacial–interglacial cycles does not exist. The lack of high-precision absolute dates severely limits our ability to identify and track the processes that led to climate shifts in the past. For MIS 7, the Penultimate Interglacial, only a few absolute dates from terrestrial and marine deposits are currently available [5–10], underscoring the need for additional data. A further difficulty is to reliably correlate sea level high stands with warm phases recorded on land [11]. Here we present the results of a study of a climate archive that contributes to the discussion about the timing and possible triggers of warm stages during the past 260 ka. The growth phases of speleothems from the high elevation Spannagel Cave, where temperature is a limiting factor controlling calcite deposition, are an indicator of warm climate and the stable oxygen and carbon isotopes provide information about environmental conditions during these intervals.

2. Study site and sample characteristics

Spannagel Cave is located in the western Zillertal Alps of Austria, approximately 30 km SSE of Innsbruck, at an elevation between 2200 and 2500 m above sea level. The area above the cave is presently ice-free but was covered by the nearby Hintertux Glacier during periods of more extensive glaciation [12]. The interior cave temperature (+1.2 to +2.2 °C, depending on the location within the 10 km cave system) shows no daily or seasonal variation and is close to the mean surface air temperature at this location (close to the 0° isotherm). As speleothems can only grow when temperatures on the surface and rock column are above the freezing point, their growth reacts sensitively to temperature shifts and no significant speleothem deposition is expected during periods when the interior cave air temperature drops below the present level by more than about 2 °C. On the other hand, the absence of calcite deposition does not necessarily imply colder climate but may instead be the result of changes in water paths and drip supply. The Jurassic calcitic marble in which the cave is cut is tectonically compressed between uraniferous granitic gneisses, a situation resulting in exceptionally high U-concentrations in the cave drip waters (up to ~33 ppb) and in the speleothems (up to ~300 ppm) [12] allowing high-precision U-series dating.

Despite cold conditions calcite speleothems are forming in Spannagel Cave today—albeit at a slow rate of ~0.04 mm/yr—as demonstrated by multiannual cave water monitoring revealing the presence of drip waters which are thermodynamically supersaturated with respect to calcite (Spötl, unpublished data). The acidity required to dissolve the marble host rock is only partially derived from pedogenic CO_2 (the ground above the cave is currently partly barren but mostly covered by alpine mats and grassland). The reaction that promotes marble dissolution in the subsurface in the absence of a major pedogenic CO_2 source is oxidation of disseminated sulfides in the overlying gneiss and to a lesser extent also in the grey marble itself. Sulfides react with oxygen-saturated seepage waters releasing dissolved sulphate and protons. The acid then dissolves the marble and secondary carbonates will start to precipitate out of solution upon entering cavities where the pCO_2 is lower than that of the solution in the narrow karst fissure network. This mode of speleothem formation by sulfide oxidation has been reported from caves elsewhere, including the alpine Castleguard Cave in Alberta [13] and Norwegian caves located near the Arctic Circle [14].

Flowstone sample SPA 59 was found in a prominent WSW–ENE trending gallery (overlying locality Lucknerhalle) in the southern central segment of Spannagel Cave at an elevation of 2400 m. This part of the cave contains abundant speleothems, predominantly flowstones and some stalagmites, none of which are actively forming today. Th/U dates from other samples in this gallery (Spötl and Mangini, unpublished data) suggest that most speleothems probably formed during MIS 7. Some of these flowstones and stalagmites broke down and are being corroded by seepage waters.

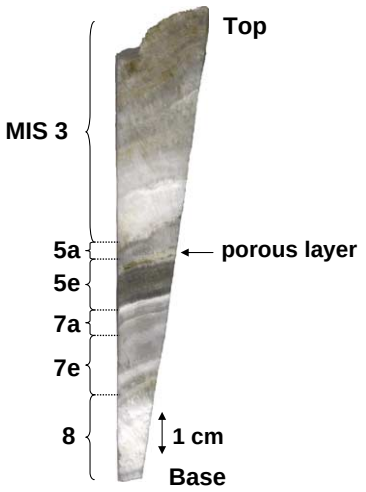

Fig. 1. Sliced flowstone SPA 59 with macroscopic hiatuses along the growth axis and assigned marine isotope stages 3 to 8 (according to the Th/U dating). The porous layer probably represents the main part of the Last Interglacial.

Sample SPA 59 is between 6 and 12 cm in diameter and reveals a complex internal stratigraphy composed of white and dark bands of coarsely crystalline low-Mg calcite (Fig. 1). A prominent dark grey layer is present near the upper half of the section and is topped by a slightly porous dissolution horizon. Additional unconformities can be identified macroscopically as well as petrographically based on the termination of columnar calcite crystals and thin layers of calcite enriched in (submicroscopic) detrital matter.

3. Methods

Thirty-seven subsamples along the growth axis of the flowstone were taken for Th/U age determination. The extraordinary high U-concentration of up to 168 μg/g helped to determine ages with high precision: the 2σ errors ranged from 0.4% at 53 ka to 2.5% at 260 ka. Small samples (less than 100 mg) were carefully cut from the sliced sample by a dedicated diamond band saw and a stainless steel slow rotation milling cutter for the high-resolution parts, respectively. Th/U measurements were performed on a thermal ionisation mass spectrometer (Finnigan MAT 262 RPQ) with a double filament technique. Analytical procedures of sample preparation are described elsewhere [15]. The results of the mass spectrometric measurements are summarised in Table 1. All ages were calculated using half-lives for ^{230}Th of 75,690 yr, for ^{234}U of 245,250 yr, and for ^{238}U of 4.4683×10^9 yr [16] and the given age errors do not include half-life uncertainties. The reproducibility of the $^{233}U/^{236}U$ double spike measured against the U-standard "112A" is 1‰ and that of the ^{230}Th spike measured against the Th-standard "HDAKT1" is 2‰. Due to a revised U-concentration of the thitherto utilised U-standard 112A, previously reported Th/U dates of samples from this cave are shifted to older ages: for MIS 3, the shift accounts for ~0.8 ka, for MIS 5e for ~3 ka, and for the beginning of MIS 7 for ~10 ka. The spike concentrations were now calibrated against the "HU-1" uraninite standard solution assuming that uraninite is at secular equilibrium for the ^{230}Th–^{234}U–^{238}U sequence. A summary of previously published [17,18] and now corrected ages can be viewed in the Supplementary online materials.

Samples for stable carbon and oxygen isotope analysis were micromilled at 100 μm intervals immediately adjacent to the Th/U samples using a computer-controlled device (Merchantek) and measured using an on-line, automated carbonate preparation system linked to a triple collector gas source mass spectrometer. Long-term precision (1σ) of δ^{13}C and δ^{18}O is 0.065‰ and 0.075‰, respectively [19]. Values are reported relative to Vienna Pee Dee Belemnite (VPDB) standard.

4. Results

4.1. Growth periods

The results of the Th/U measurements indicate that the flowstone formed between 261.4 ± 6.5 and 52.9 ± 0.2 ka. Calcite deposition was repeatedly interrupted as shown by steps in the age profile (Fig. 2) and the presence of petrographically identified growth hiatuses (Fig. 1). Furthermore, the growth phase boundaries are characterised by local minima in the stable isotope profile.

The formation of spelean calcite indicates temperatures above the freezing point at this high Alpine site and the flowstone therefore serves as a record of warm periods. We associate these warm periods on

Table 1
Mass-spectrometric U-series ages, $^{234}U/^{238}U$ activity ratios, and isotope concentrations of flowstone SPA 59

Distance from base		$\delta^{234}U$		Conc. ^{238}U		Conc. ^{232}Th		Conc. ^{230}Th		Age		MIS
(mm)	± (mm)	(‰)	± (‰)	(μg/g)	± (μg/g)	(ng/g)	± (ng/g)	(pg/g)	± (pg/g)	(ka)	± (ka)	
1.4	2.5	25.81	1.83	161.91	0.18	2.86	0.01	2479.73	14.63	257.9	6.5	8
5.4	1.5	30.72	2.35	164.76	0.23	0.96	0.01	2547.18	13.25	261.4	6.5	"
7.4	1.5	31.21	1.57	167.54	0.10	0.37	0.00	2577.93	5.16	255.9	2.8	"
19.9	2.5	56.01	2.79	98.52	0.16	0.40	0.00	1543.09	4.78	249.0	4.5	"
23.9	1.0	44.39	1.78	95.88	0.11	0.23	0.00	1467.27	2.64	236.4	2.4	7e
23.9	1.0	56.42	2.03	79.47	0.10	117.32	0.22	1233.76	3.33	236.4	4.4	"
29.4	0.5	45.46	2.45	100.25	0.15	<0.1	x	1530.33	3.06	233.3	3.1	"
29.7	2.5	46.29	4.22	98.07	0.28	<0.1	x	1496.33	3.29	232.2	4.9	"
33.4	0.5	39.75	2.75	46.14	0.07	1.82	0.00	695.88	1.67	229.2	3.4	"
35.1	2.2	51.48	2.09	22.82	0.03	45.34	0.06	341.98	0.72	214.8	2.3	x
37.4	1.0	82.46	2.19	64.67	0.07	105.02	0.23	966.86	3.09	193.1	2.1	7a
37.5	2.5	80.36	2.79	51.47	0.08	62.26	0.10	777.18	1.79	199.6	2.3	"
39.4	1.0	83.352	2.76	74.82	0.13	4.05	0.01	1117.60	3.91	192.1	2.5	"
41.9	1.0	85.24	2.77	81.80	0.14	127.65	1.07	1051.43	10.41	136.7	2.8	5e
42.9	1.0	91.33	2.47	54.16	0.08	122.82	0.37	688.53	2.20	132.1	1.1	"
44.9	1.0	85.58	1.85	55.06	0.06	85.77	0.29	703.69	3.80	135.0	1.5	"
49.4	0.5	71.32	1.98	28.22	0.04	346.70	0.42	348.43	0.91	129.9	0.9	"
50.4	0.5	74.59	1.85	24.70	0.02	132.39	0.17	307.31	0.61	131.1	0.8	"
52.0	1.0	73.55	2.21	10.45	0.01	219.76	0.44	129.32	0.53	129.6	1.2	"
52.9	2.0	76.53	3.18	16.51	0.02	103.53	0.29	190.89	0.86	114.4	1.2	x
55.3	1.0	43.62	5.28	13.60	0.03	28.57	0.21	133.86	1.49	92.9	1.8	x
55.5	1.0	34.61	1.67	38.59	0.03	74.96	0.15	353.65	0.88	84.6	0.4	5a
56.4	0.5	44.69	4.60	49.09	0.14	34.10	0.10	435.32	1.13	79.3	0.7	"
56.9	0.5	23.26	2.24	62.22	0.10	7.94	0.02	526.72	1.26	76.6	0.4	"
57.4	0.5	26.70	4.17	47.90	0.12	5.54	0.03	409.27	2.25	77.3	0.9	"
58.9	1.0	22.70	3.21	37.21	0.04	11.24	0.07	315.13	2.62	76.7	1.0	"
59.9	1.0	18.29	1.67	24.82	0.02	20.61	0.04	204.48	0.67	74.3	0.4	"
60.9	1.0	36.20	7.06	21.14	0.09	51.89	0.14	175.10	1.16	72.8	1.2	"
64.9	2.0	23.06	2.89	103.36	0.21	8.64	0.01	729.31	1.46	59.6	0.3	3
66.2	1.2	22.16	1.90	134.08	0.15	12.42	0.01	947.98	1.42	59.8	0.2	"
71.6	1.7	24.48	2.97	138.87	0.28	1.19	0.00	988.41	2.97	60.2	0.4	"
72.9	2.0	17.61	4.83	142.16	0.50	1.92	0.00	998.21	2.00	59.7	0.5	"
82.4	2.5	22.65	5.79	57.84	0.22	0.56	0.01	392.54	5.18	56.7	1.1	"
91.9	2.0	30.06	3.75	54.50	0.10	1.53	0.01	366.19	3.19	55.4	0.7	"
99.4	2.5	18.94	2.02	50.28	0.07	2.99	0.02	329.67	1.58	54.5	0.4	"
107.4	2.5	15.18	2.03	29.76	0.04	79.32	0.10	190.21	0.36	52.9	0.2	"
112.1	2.2	20.49	2.03	29.81	0.04	71.56	0.20	197.52	1.09	55.0	0.4	"

All results are given versus distance from flowstone base with 2σ errors. Detrital correction was performed assuming a $^{232}Th/^{238}U$ mass ratio in the detritus of 3.8 [20] and led to negligible correction (<0.1 ka), apart from ages 131.1 ka (−0.1 ka), 129.9 ka (−0.3 ka), 129.6 ka (−0.6 ka), and 114.4 ka (−0.2 ka).

land with sea level high stands from the $\delta^{18}O$ values of deep sea sediments [3,4], being aware of their formal and relevant difference. This is demonstrated for the Last Interglacial complex, when the sea level reached maximum values ~2 ka before the beginning of interglacial conditions on land and when vegetation indicating warm climate continued well into MIS 5d [11,21]. However, it seems appropriate to label the warm periods on land according to their marine counterparts, i.e. the marine isotope stages, as long as there is no widely accepted entity for terrestrial sequences. In that sense, the growth phases from Spannagel reproduce the main features of other palaeoclimatic reconstructions of the respective time intervals but also illustrate some important differences (Fig. 3). Apart from MIS 5c and 7c, all the other warm phases were identified in the flowstone and some important dates are added, especially for

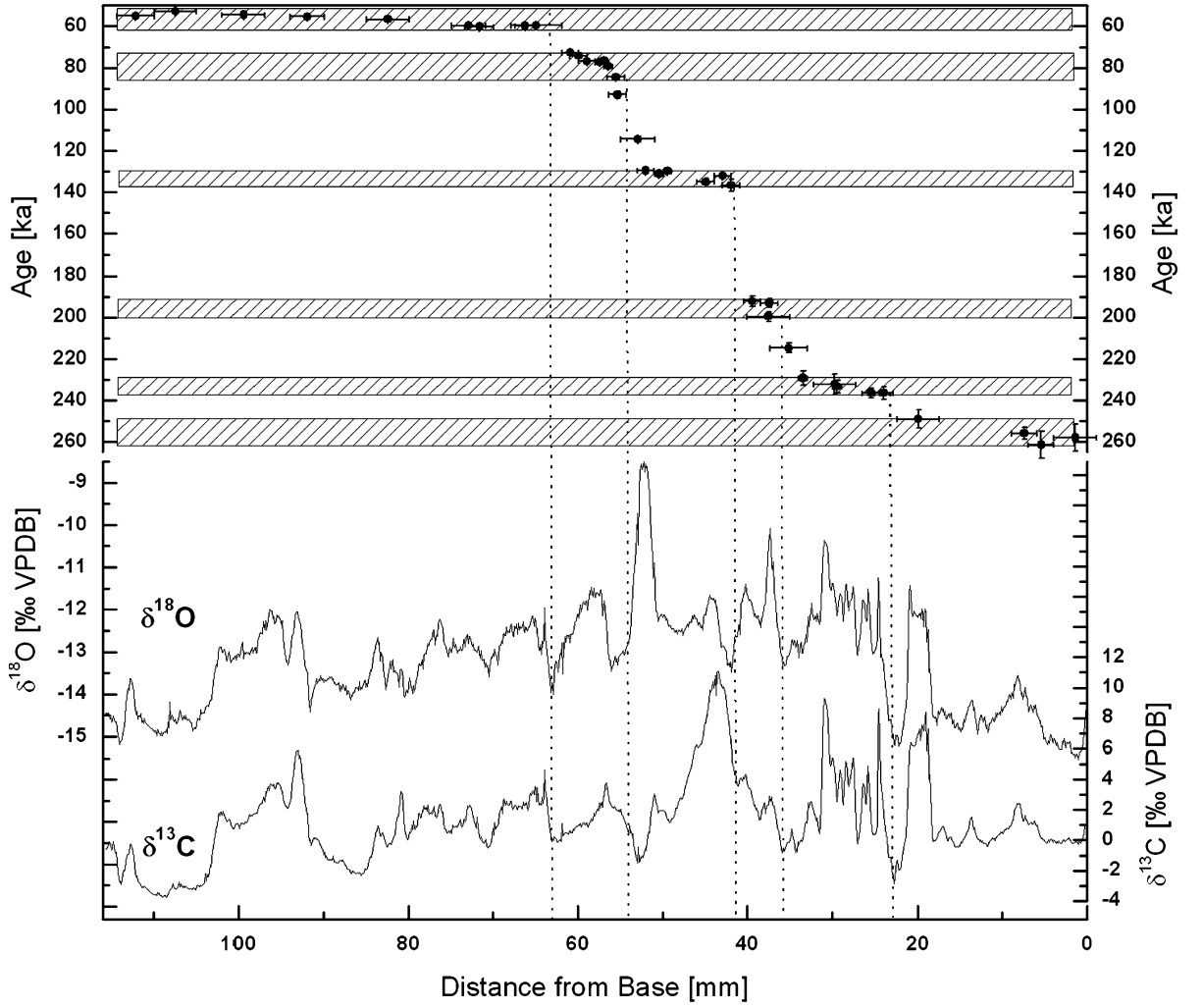

Fig. 2. Dating results and stable isotope profiles of flowstone SPA 59. All Th/U ages are given with 2σ errors. Error bars in x-direction are determined by visual inspection and indicate the uncertainty in correlating the stable isotope profile to the Th/U samples. The distinct growth periods are indicated by hatched boxes. Steps in the age profile and macroscopic hiatuses reveal that speleothem growth was repeatedly interrupted (shown by vertical dashed lines indicating the positions of growth phase boundaries).

the Penultimate Interglacial, where absolutely dated records are rare.

The growth of flowstone SPA 59 commenced at 261.4 ± 6.5 ka and continued until a first interruption at 249.0 ± 4.5 ka, thus the first section corresponds to MIS 8 according to SPECMAP [3]. In order to avoid confusion, we label this first growth phase as a warm event within MIS 8. No macroscopic hiatus is visible within this section. After the first growth stop, which is marked by a brownish hiatus, calcite growth recommenced at 236.4 ± 2.4 ka and about 14 mm of mainly translucent calcite formed until 229.2 ± 3.4 ka. This second growth phase is assigned to MIS 7e; it is characterised by a major whitish hiatus and a few indistinctive minor hiatuses, the ages of which could not be resolved by our dating technique. The MIS 7c warm stage is not present in our record. According to the palaeotemperature record DH-11, a 36-cm-long core of vein calcite from Devils Hole, Nevada [25] and two Th/U dated sediment cores from the Bahamas [7], MIS 7c commenced at ~215 ka, about 5 ka later than defined by the SPECMAP curve. Both the Devils

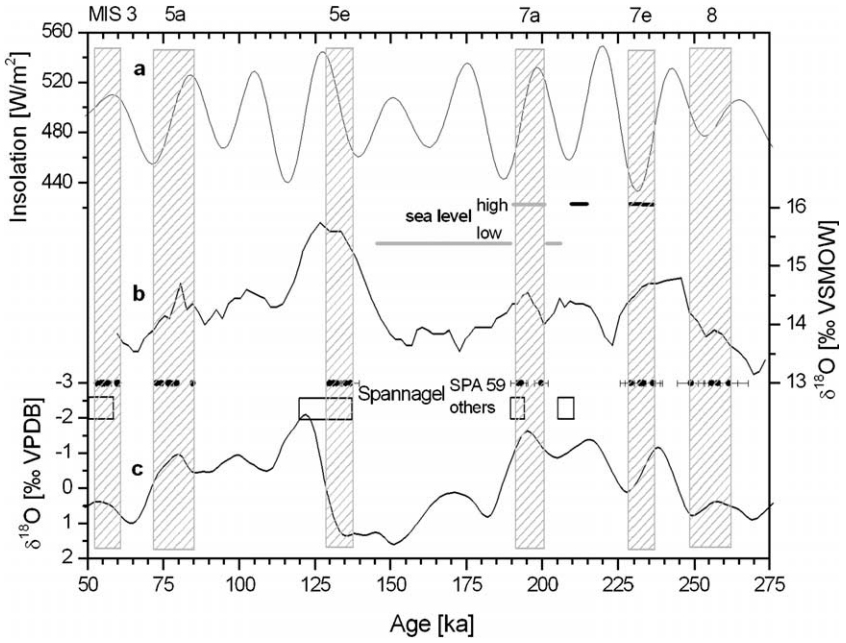

Fig. 3. Growth phases of flowstone SPA 59 from Spannagel Cave (large hatched boxes; the smaller boxes indicate the growth phases of other investigated speleothems of Spannagel Cave, comprising of samples SPA 52 [17], SPA 50 [18], SPA 51 [22], SPA 126 [23], SPA 49 [24]), compared with 60° N summer insolation (a), the δ^{18}O record from groundwater calcite at Devils Hole, Nevada [25] (b), and the stacked δ^{18}O record from marine calcite (SPECMAP) [3] (c). Also shown are 34 Th/U ages with 2σ error bars. Three additional points interpreted as mixing ages were omitted. Growth phases of a submerged stalagmite from Argentarola Cave (Italy) are indicated by two grey horizontal bars [6], representing a sea level of less than -18.5 m relative to the present value. The growth interruption indicates that the sea level was above this value (i.e. warm climate) (upper grey bar). Additionally, warm stages derived from Th/U dated slope sediments from the Bahamas [7] are indicated as black horizontal bars.

Hole record and the sea level record derived from submerged speleothems from Argentarola Cave (Italy) [6] place the end of MIS 7c at about 206 ka. One age (215 ka) of SPA 59, which would fall into this period, was discarded because of obvious admixture of material from the next hiatus. Similar to the MIS 8/7e boundary, the transition between MIS 7e and 7a is marked by a distinct hiatus in SPA 59, where calcite deposition recommenced at 199.6 ± 2.3 ka. MIS 7a is represented by a section of 6 mm and the youngest calcite of MIS 7a was dated 192.1 ± 2.5 ka.

The Last Interglacial part consists of a thin porous layer of about 12 mm thickness and is therefore not suitable for high-resolution investigations, in contrast to flowstone SPA 52 and stalagmite SPA 50 retrieved from the same cave [18]. The Last Interglacial layer can be subdivided into four distinct layers of about 3 mm thickness each. The first (oldest) and third layer consist of translucent clear calcite, the second one of brownish opaque carbonate, and the uppermost (youngest) unit is porous and laminated (highlighted in Fig. 1). In general concordance with the revised results from SPA 50 and SPA 52, deposition commenced at 136.7 ± 2.8 ka (first layer). The youngest layer of the MIS 5e section yielded an age of 129.6 ± 1.2 ka (third layer). The fourth layer, probably representing the main part of the Last Interglacial, was not dated due to its high porosity. A layer of 9 mm thickness above the Last Interglacial section represents MIS 5a, as shown by ages ranging from 84.6 ± 0.4 to 72.8 ± 1.2 ka. Two points in close proximity to the hiatus ensuing the porous section of the Last Interglacial, which were dated at 114.4 and 92.9 ka, are interpreted as mixing ages and are therefore discarded.

The youngest growth phase of flowstone SPA 59 can be assigned to MIS 3, yielding ages between 60.2 ± 0.4 and 52.9 ± 0.2 ka. This calcite contains about 10 faint brownish bands close to the top of the flowstone.

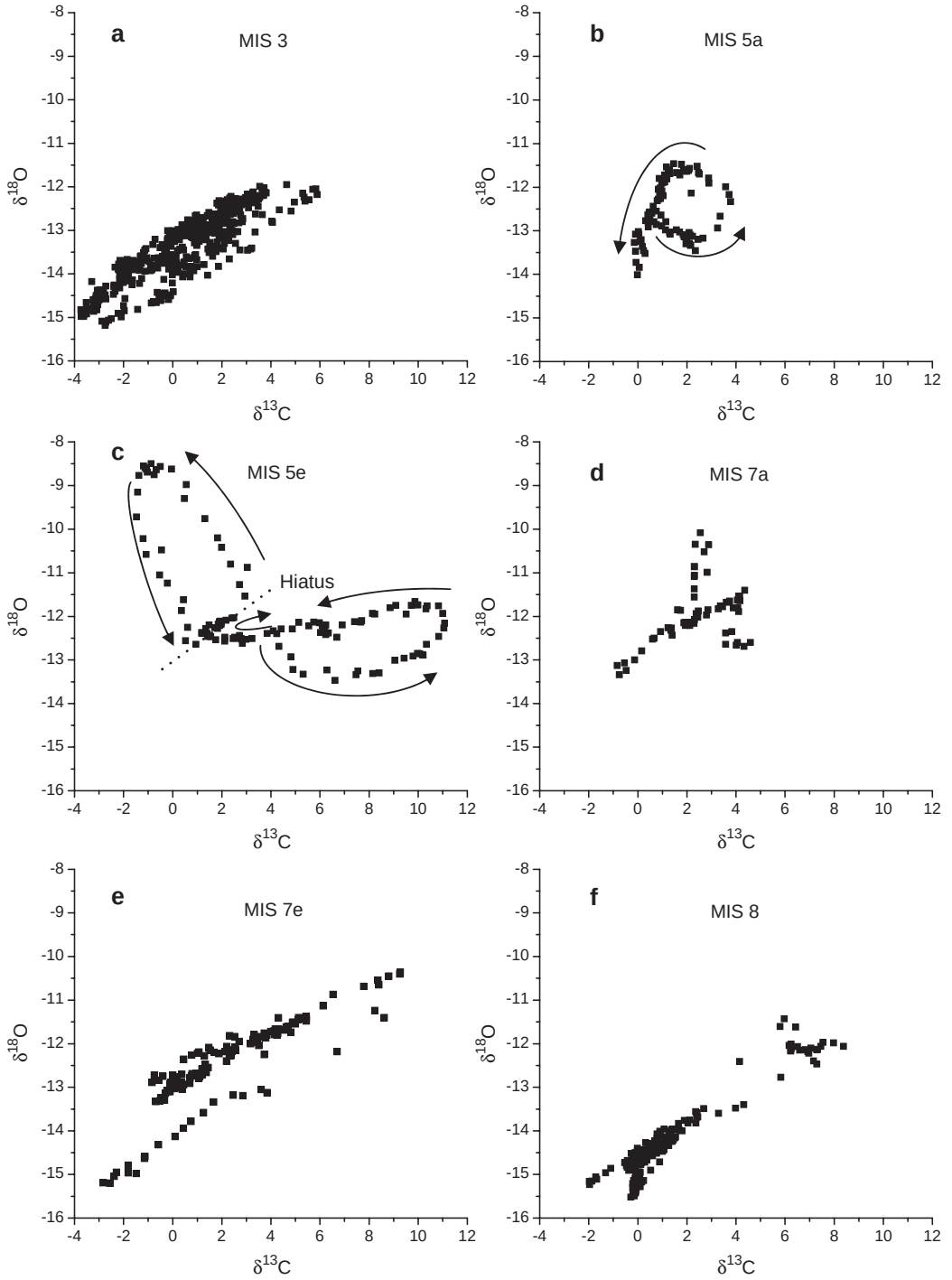

Fig. 4. Correlation between $\delta^{13}C$ and $\delta^{18}O$ for each growth phase. The arrows in plots b and c mark the progression of the isotope ratios during the respective growth phase.

4.2. Stable isotope profile

Both the $\delta^{18}O$ and $\delta^{13}C$ values show large variations throughout the entire profile taken along the growth axis of the flowstone. A weak long-term trend is visible in the $\delta^{18}O$ profile, with a slight increase from ~−15‰ VPDB at the bottom of the flowstone, corresponding to MIS 8, to ~−12‰ (lower layer of MIS 5e) and −8.5‰ (upper layer of MIS 5e), respectively, in the middle part, followed by a decrease to the initial values at the top of the flowstone (MIS 5a and MIS 3). No long-term trend is visible for the $\delta^{13}C$ profile, which shows a mean value of around +1‰ VPDB. The short-term variability, with amplitudes of ~1‰ to 4‰ ($\delta^{18}O$) and ~3‰ to 11‰ ($\delta^{13}C$), respectively, is high in comparison to other speleothems and the local minima of the stable isotope profile can be correlated to petrographic hiatuses. Consistent with our dating results, each segment between two hiatuses represents a warm stage and the hiatuses are marked both by steps in the depth-age profile and spikes in the stable isotope profile. While the low $\delta^{18}O$ values toward the hiatuses may be explained by the enhanced influx of depleted glacial melt water and lower $\delta^{18}O$ of meteoric precipitation during cooler periods, the cause for the local minima in the $\delta^{13}C$ profile remains unclear. Three remarkable features characterise the stable isotope profile of flowstone SPA 59: high values of $\delta^{13}C$ of up to +11‰, high variability with large amplitudes in both $\delta^{18}O$ and $\delta^{13}C$, and covariance between both isotope ratios over major parts of the flowstone profile. Comparing $\delta^{13}C$ and $\delta^{18}O$ values for individual growth periods (Fig. 4) illustrates two interesting aspects: (1) in 4 out of 6 growth periods, the correlation between $\delta^{13}C$ and $\delta^{18}O$ is high. The respective correlation coefficients are 0.90 (MIS 3), 0.42 (MIS 7a), 0.88 (MIS 7e), and 0.94 (MIS 8) and the gradients are nearly constant within one layer; and (2) during MIS 5e and MIS 5a the relationship between $\delta^{13}C$ and $\delta^{18}O$ values is more complex. Two distinct loops subdivided by a hiatus represent the first growth phase of MIS 5e and the presumed "classical Eemian", respectively (Fig. 4c). A weak positive correlation between $\delta^{13}C$ and $\delta^{18}O$ can be observed for the first part of the MIS 5e layer and a weak negative correlation in the second, the main Last Interglacial part. A deviation from the straightforward positive correlation can also be seen within the MIS 5a growth layer.

5. Discussion

5.1. Growth periods

The first growth period of flowstone SPA 59 as early as 261.4 ± 6.5 ka is well within MIS 8 as defined by the orbitally tuned deep sea oxygen-isotope chronology [4]. Alternatively, it marks an early onset of MIS 7e, i.e. Termination III. This would—within error—be in agreement with the results from the Th/U dated vein calcite from Devils Hole [25], which shows an increase in $\delta^{18}O$ values at about the same time. The Devils Hole chronology of MIS 7 and 8, however, is based only on four age control points, ranging between 211.0 ± 2.9 and 285.7 ± 3.5 ka [2], thus limiting the significance of this sample during this period.[1] The 60° N summer insolation shows a second order peak at ~263 ka which may at least have contributed to the warming observed in the high Alps, comparable to the interstadial conditions during MIS 3. More data are clearly needed to enlighten the climate during MIS 8. Th/U-ages derived from the Bahamas slope sediments suggest that full interglacial conditions of MIS 7e lasted from ~237 to 228 ka [7], which fits remarkably well to the second growth phase of SPA 59, from 236.4 ± 2.4 to 229.2 ± 3.4 ka. Thus, both records indicate full interglacial conditions clearly later than the orbitally tuned SPECMAP time scale, which places Termination III at ~245 ka. Additional support for the timing of this warm phase comes from the U-series dated flowstone DWBAH from the submerged Lucayan Caverns, Grand Bahamas Island, where a hiatus at about 235–232 ka indicates a sea level higher than −10 to −15 m in comparison to the present value [9]. According to the results from newly processed open-system ages from Barbados corals

[1] The suitability of the Devils Hole core as a sensitive record of global climate has been questioned [8,26,27], and one severe challenge attests that the record rather represents regional temperatures responding to the weakening of the cold California Current during peak glacial conditions [28]. Yet the fact that many features of the Devils Hole record are reproduced by a large number of independent climate archives reinforces its value as a precious data set.

[10], however, sea level was within today's range from ~243 to 239 ka, i.e. markedly earlier than indicated by our record. These coral dates also indicate a brief 20 m sea level drop at about 240 ka, suggesting either rapid climate changes during that period or an uncertain age control for this single data point. Regarding the stability of the climate of MIS 7e, the one distinct hiatus in SPA 59 and the few other minor hiatuses within this speleothem section may indicate unstable conditions but might also be the result of local hydrological processes.

The absence of calcite from MIS 7c in our flowstone sample is most likely the result of a change in the local hydrological regime rather than climatic conditions unfavourable of calcite precipitation. Local site conditions can bias the growth of single speleothems (and in particular of flowstones) [29] and therefore it is crucial to examine the growth of several coeval speleothem samples to achieve a meaningful palaeoclimate reconstruction. Indeed, the previously studied flowstone sample SPA 52 formed in the northern branch of the cave, 550 m apart from and 55 m deeper than sample SPA 59, during that time. A succession of 39 mm of calcite was deposited after 211.4 ± 2.4 ka (updated chronology of [17]; see Supplementary online materials) consistent with the timing of MIS 7c according to the Devils Hole chronology [2].

The beginning of MIS 7a at 199.6 ± 2.3 ka derived from SPA 59 is concordant with results from the submerged speleothems from Argentarola Cave and the SPECMAP record, both indicating a high sea level between 202 and 190 ka. This result is corroborated by 3 Th/U dates from Barbados corals that grew during MIS 7a and which recorded sea levels within today's range at 200.8 ± 1.0, 200.1 ± 1.2, and at 193.5 ± 2.8 ka [8]. Also the end of the warm period is confirmed by the SPA 59 record with a Th/U age of 192.1 ± 2.5 ka. This value is indistinguishable from the top age of the MIS 7 package in sample SPA 52 of 188.7 ± 2.8 ka (updated chronology of [17]; see Supplementary online materials), providing independent confirmation from a second sample of the same cave for the end of warm phase MIS 7a at ~190 ka.

In agreement with other absolutely dated climate archives [25,30–32], the beginning of MIS 5e was dated at 136.7 ± 2.8 ka, ~7 ka earlier than suggested by the SPECMAP curve. In a previous study we reported a basal age of 135 ± 1.2 ka for the onset of speleothem deposition in flowstone SPA 52 [17], overlying the MIS 6 hiatus. Within this ~4 cm interval 8 further ages between 133.6 ± 2.2 and 129.2 ± 1.8 ka were determined [17] and these have been revised using our recalculated value for the spike (see Supplementary online materials). Fig. 5 shows the revised age distribution as well as a new Th/U analysis from the lowermost 2 mm of this layer.

The diagram shows that within this interval (Unit 3) there is only a weak stratigraphic relationship and significant age variability. We place the onset of calcite precipitation close to ~137 ka which is within the age uncertainties of the three previously oldest dates and which is consistent with a new measurement carefully taken from the basal calcite above hiatus H2 (136.8 ± 0.9 ka). This age is comparable to the date of sample SPA 59 (136.7 ± 2.8 ka) and only slightly older than the basal age of stalagmite SPA 50 (updated chronology of [18]; Supplementary online materials), i.e. 133.6 ± 1.6 ka. In essence, these three samples strengthen our previous interpretation of an early start of the penultimate deglaciation at this high-altitude cave site and suggest an even earlier timing (close to 137 ka). Such an early start of the Last Interglacial is difficult to reconcile with a forcing by increased 60° N summer insolation, which peaks at 128 ka. These data, however, are in agreement with Th/U-dated evidence of a high sea level at that time [30–32]. In addition, recent stalagmite data point toward a warm and wet (monsoonal) climate in SE China at ~137 ka (R.L. Edwards, personal communication, 2004).

The low temporal resolution of sample SPA 59 does not permit insights into the structure of the Last Interglacial (i.e. the creation of a plot 'isotope profile versus age'), but the complex layering suggests that the Last Interglacial karst hydrology—and possibly also climate—was variable. The lack of calcite that dates from the "plateau" of MIS 5e (lasting from ~128 ka until 116 ka [33]) in this record and thus from the warmest period of the Last Interglacial is attributed to local dissolution processes that affected flowstone SPA 59 probably as a result of high discharge of rather dilute seepage water. The high amount of insoluble residue in the Last Interglacial calcite as well as the observation that speleothems from this part of the cave are currently being corroded by modern seepage waters corroborates this interpretation. Peak interglacial conditions are, however, recorded in flowstone SPA 52 by a conspic-

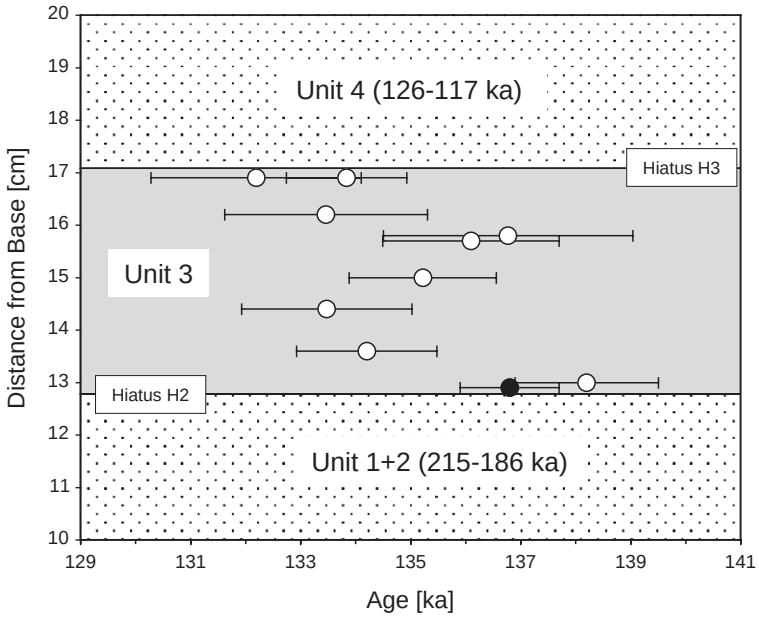

Fig. 5. Diagram showing the revised Th/U results of the early MIS 5e layer in flowstone SPA 52. Open circles are those of Fig. 2 in [13] and the filled circle shows a new measurement. The age ranges of the layers beneath and above Unit 3 include the maximum 2σ age uncertainties.

uous translucent layer (Unit 4 in Fig. 5) formed between 124.5 ± 0.9 and 118.5 ± 2.0 ka (updated chronology of [17]; see Supplementary online materials). Nearby stalagmite SPA 50 also shows a series of growth phases with inclusion-poor calcite between 128.5 ± 1.3 and 120.8 ± 0.9 ka (updated chronology of [18]; Supplementary online materials).

The reason for the absence of calcite deposition during MIS 5c may be a strong glacial advance during the preceding MIS 5d stadial in the Alpine region, when the sea level dropped by ~50–70 m [34], resulting in the warming of MIS 5c being insufficient in length in order to produce ice-free conditions above Spannagel Cave. Alternatively, MIS 5c may not have been as warm as the other interstadials recorded from SPA 59, as indicated by sea-surface temperature reconstructions from northeast Atlantic sediments [35]. It is also possible that hydrological conditions were unfavourable of calcite deposition for a variety of reasons, so that the absence of growth does not necessarily imply colder climate.

MIS 5a calcite records conditions conducive of speleothem deposition between 84.6 ± 0.4 and 72.8 ± 1.2 ka (Fig. 3). These dates agree well with the results derived from speleothem and travertine deposits from northeastern Brazil, which indicate wet conditions in this region synchronous with periods of weak East Asian summer monsoon and cold periods in Greenland before 86.5 ± 0.4 ka [36]. Speleothem growth in the Oman' Hoti Cave evidences a northward shift of the limit of the monsoonal rainfall over the Arab Peninsula between 82.5 ± 1.2 and 77.6 ± 2.5 ka [37], thus representing the warmest portion of MIS 5a. The somewhat later initiation and earlier cessation of calcite growth in Oman may indicate a higher threshold in response to climate warming in that region in comparison to the Alps; this feature is also apparent during Termination II, when speleothem formation in Hoti Cave does not commence before 131 ka, ~6 ka later than in Spannagel Cave (Holzkämper et al., unpublished data). According to the reconstruction from Barbados corals that show no evidence of diagenesis the sea level reached -15.5 ± 2.5 m relative to the present value at 83.3 ± 0.3 ka [8], remained relatively high until at 76.2 ± 0.4 ka (-24 m), and dropped rapidly to -81 m 70.8 ka ago [38]. The comparatively late speleothem formation in the Alps at a time when the sea level was already falling indicates that severe cooling and ice build-up was in progress before the speleothem growth came to an end. One explanation

could be a warm period that interrupted the climatic cooling after ~76 ka. Indeed, the deep sea sediment core MD99-2331 retrieved from the northwestern Iberian margin indicates climate cooling after about 76 ka [39] but also shows evidence of a brief warm event close to the transition to the MIS 4 stadial. This interpretation is consistent with a hiatus at ~73 ka separating two brief growth periods at about 74 and 72 ka in the Brazil record [36], as well as with a new compilation of data from Barbados corals which shows a sea level drop after about 78 ka followed by a second peak centred at 73.9 ± 1 ka [10]. We note that our youngest date is indistinguishable from a top Th/U date of a Norwegian stalagmite from Rana Cave (73.3 ± 0.4 ka) located near the Arctic Circle. This stalagmite stopped growing immediately afterwards as a result of valley glaciers advancing across the area above the cave and associated flooding of the cave by melt water during MIS 4 [40]. Conditions most likely changed dramatically afterwards (glacier expansion) and no speleothems of MIS 4 age have been found in Spannagel Cave so far. The precise nature and extent of this MIS 4 glacier advance in the Alps is still poorly known, but recent optically stimulated luminescence dates suggest that the valley glaciers may have reached the northern alpine foreland [41].

The topmost calcite layer of SPA 59 formed between 60.2 ± 0.4 and 52.9 ± 0.2 ka, i.e. during MIS 3 (Fig. 3). The O isotope profile of this layer suggests significant variability (Fig. 2) probably reflecting Dansgaard–Oeschger climate dynamics. Such cycles have been reported from a neighbouring cave in the Spannagel area, Kleegruben Cave, based on O isotope data [24]. Although SPA 59's very slow growth rate during this interval (~6 mm/ka) and the possible presence of hiatuses render a detailed correlation with the stalagmite record from [24] difficult, the prominent interval of relatively high $\delta^{18}O$ values ~92 to 102 mm above the base (Fig. 2) probably represents Greenland Interstadial 14. We also note that the O isotope amplitude is comparable to the ~2‰ variability observed in the stalagmite from Kleegruben Cave [24]. Flowstone SPA 59, which formed at an altitude even 250 m higher than this stalagmite, therefore supports the previous interpretation of temperatures above the freezing point during MIS 3 [24].

In essence, the timing of growth intervals in flowstone SPA 59 is only partially consistent with the model of orbital forcing of late Quaternary climate changes. When viewing the timing of the growth periods equivalent to MIS 7a, 5a, and 3, the theory of orbital climate forcing seems to be corroborated, as speleothem growth sets in when northern summer insolation is at or close to its maximum. However, when examining the overall timing of speleothem growth intervals in Spannagel Cave (Table 2), we do not find a concordance with northern summer insolation, as shown by growth initiation at second order peaks (MIS 8), at insolation minima (MIS 5e), and at decreasing insolation (MIS 7e). We conclude that additional triggers and/or mechanisms must have been involved in initiating climate variations over the past 260 ka.

5.2. Stable isotope profile

In Spannagel, a key process that leads to the formation of speleothems is the dissolution of the marble

Table 2
Timing and thickness of growth phases in speleothems from Spannagel Cave

MIS	SPA 50		SPA 52		SPA 59	
	Age (ka)	Thickness (mm)	Age (ka)	Thickness (mm)	Age (ka)	Thickness (mm)
8					261–249	22
7e					236–229	14
7c			211–206	39		
7a			195–189	97	200–192	6
5e	134–121	252	137–118	79	137–130	12
5a					85–73	9
3					60–53	48

The dates for SPA 50 and SPA 52 are revised from [18] and [17].

by sulfuric acid evolved from the oxidation of pyrite [12]. Additionally, a slight increase in temperature that glacial melt waters experience upon their journey into the cave could have enabled speleothem growth [42], but as the temperature in the cave is only marginally higher than the long-term mean annual air temperature, this process is regarded as negligible. Pedogenic CO_2 contributed to carbonate dissolution during peak interglacial conditions, where comparably low $\delta^{13}C$ values of −3‰ to −4‰ indicate the presence of a vegetation cover above the cave. Values as low as −8.6‰ are recorded in Holocene stalagmites [43]. However, apart from the warmest portions of the growth phases, there was only minimal vegetation above the cave, so that the $\delta^{13}C$ values of the speleothems were mainly influenced by the host rock with values of +2‰ to +3‰ [12]. Carbonates originating from a purely atmospheric CO_2 source can reach maximum $\delta^{13}C$ values of +6‰ at 2 °C under isotopic equilibrium [12]. The extraordinary high $\delta^{13}C$ values of up to +11‰ must consequently be attributed to kinetic fractionation prior to or during carbonate precipitation.

$\delta^{18}O$ values in speleothems are controlled by the isotopic composition of meteoric precipitation and by the conditions during which calcite is precipitated from the drip water. If we presume constant $\delta^{18}O$ values of precipitation during each growth phase and equilibrium fractionation during calcite precipitation, the observed short-time variations of 1‰ to 4‰ would translate into 4 to 16 °C temperature fluctuations [44]. As today's temperature in the cave is about +1.8 °C and speleothems can only form above the freezing point, such temperature variations are extremely unlikely. Therefore, factors other than the cave temperature must be responsible for such large variations. The simultaneous enrichment of $\delta^{18}O$ and $\delta^{13}C$ strongly suggests that kinetic fractionation is a likely explanation for the observed trends [45].

Speleothems, whose stable isotope partitioning was partially controlled by kinetic fractionation, are widely regarded as less useful palaeoenvironmental archives than those that formed under equilibrium conditions. Kinetic isotope effects arise from the preferential loss of the light isotopes of C and O from the solution during rapid irreversible loss of CO_2 [46]. This implies that an enhanced degassing of CO_2 leads to enrichment in both ^{13}C and ^{18}O in the precipitating carbonate. Rapid loss of CO_2 can be the result of a high gradient between the aqueous carbon dioxide and the cave atmosphere and of a thin water film on the surface of a speleothem. Both conditions may prevail under comparably dry conditions, i.e. when only small amounts of water penetrate the cave, enriched in CO_2 due to long residence times in the overlying fissure network of the host rock. Which processes were actually responsible for the strong kinetic fractionation in the Spannagel Cave, however, is currently subject of ongoing investigations, i.e. monitoring of the isotopic composition of the drip water and cave climate.

As a consequence, the oxygen and carbon isotope profiles of the growth phases representing MIS 3, 7a, 7e, and 8 may indicate very low seepage water discharge onto the flowstone's surface. The more complex behaviour during growth phases MIS 5e and 5a suggests that other hydrological and/or climatic conditions prevailed. While the oldest growth layer of MIS 5e shows a weak positive correlation between the carbon and oxygen isotopes (lower right part of Fig. 4c), we observe a negative correlation between $\delta^{18}O$ and $\delta^{13}C$ in the second layer (upper left part of Fig. 4c). The rise of $\delta^{18}O$ values in the second layer from −12‰ to −8‰ can be attributed to the decreasing influence of isotopically depleted glacial melt water in comparison to warm-climate precipitation. This course is also seen in the Last Interglacial sections of flowstone SPA 52 [17] and stalagmites SPA 50 and SPA 51 [18,22]. Simultaneously, increasing vegetation density above the cave led to pedogenic CO_2 enrichment in the soil resulting in a modest reduction of $\delta^{13}C$ values due to depleted values of CO_2 of organic matter mixing with marble-derived bicarbonate. The lack of a positive relationship between C and O isotope values in this peak MIS 5e interval strongly suggests that this calcite probably formed under near-isotopic equilibrium conditions. With the possible exception of MIS 5a, where the correlation between $\delta^{18}O$ and $\delta^{13}C$ is also poorly developed (Fig. 4b), MIS 5e is the only period of largely kinetic-free precipitation (also shown in flowstone SPA 52 [22]). We ascribe this to a switch in groundwater discharge brought about by the prevailing warm and humid interglacial climate, probably the warmest interval during the past 260 ka.

6. Conclusions

Our dataset shows that calcite deposition at Spannagel Cave occurred during interglacial periods over the past 260 ka. Given the inherent spatial variability of seepage flow routes, sheet-like speleothems (flowstones) are more prone to hiatuses than stalagmites. We therefore regard the presence, but not the lack, of calcite from a particular time interval as a reliable climatic indicator. This is clearly demonstrated by the fact that flowstone sample SPA 59 shows no record of the interstadial warm phase corresponding to MIS 7c, whereas a parallel sample (SPA 52) from a different part in the same cave does. Taken together, the growth phases of speleothems from Spannagel Cave give a robust record of warm periods in this climate-sensitive alpine environment which is consistent with Th/U-dated marine records. The timing of the onset and termination of these speleothem growth phases, however, can only partly be explained by Milankovitch forcing and additional triggers and/or mechanisms have to be considered.

Acknowledgments

We thank M. Wimmer for her excellent work in the stable isotope laboratory. Helpful comments by D. Richards, F. McDermott and an anonymous reviewer significantly improved the quality of the manuscript. Funding for this study was provided by the DEKLIM program of the German Federal Ministry for Education and Research and the Austrian Science Fund (START Y122-GEO).

Appendix A. Supplementary data

Supplementary data associated with this article can be found, in the online version, at doi:10.1016/j.epsl.2005.06.002.

References

[1] J.R. Petit, J. Jouzel, D. Raynaud, N.I. Barkov, J.-M. Barnola, I. Basile, M. Bender, J. Chappellaz, M. Davis, G. Delaygue, M. Delmotte, V.M. Kotlyakov, M. Legrand, V.Y. Lipenkov, C. Lorius, L. Pepin, C. Ritz, E. Saltzman, M. Stievenard, Climate and atmospheric history of the past 420,000 years from the Vostok ice core, Antarctica, Nature 399 (1999) 429–436.

[2] I.J. Winograd, J.M. Landwehr, K.R. Ludwig, T.B. Coplen, A.C. Riggs, Duration and structure of the past four interglaciations, Quaternary Science Reviews 48 (1997) 141–154.

[3] J. Imbrie, J.D. Hays, A. McIntyre, A.C. Mix, J.J. Morley, N.G. Pisias, W.L. Prell, N.J. Shackleton, The orbital theory of Pleistocene climate: support from a revised chronology of the marine $\delta^{18}O$ record, in: A. Berger, J. Imbrie, J. Hays, G.J. Kukla, E. Saltzman (Eds.), Milankovitch and Climate, Reidel, Boston, 1984, pp. 269–305. Part I.

[4] D.G. Martinson, N.G. Pisias, J.D. Hays, J. Imbrie, T.C. Moore Jr., N.J. Shackleton, Age dating and the orbital theory of the ice ages: development of a high-resolution 0 to 300,000-year chronostratigraphy, Quaternary Research 27 (1) (1987) 1–29.

[5] K.R. Ludwig, K.R. Simmons, B.J. Szabo, I.J. Winograd, J.M. Landwehr, A.C. Riggs, R.J. Hoffman, Mass-spectrometric ^{230}Th–^{234}U–^{238}U dating of the Devils Hole calcite vein, Science 258 (1992) 284–287.

[6] E. Bard, F. Antonioli, S. Silenzi, Sea-level during the Penultimate Interglacial period based on a submerged stalagmite from Argentarola Cave (Italy), Earth and Planetary Science Letters 196 (2002) 1–12.

[7] L.F. Robinson, G.M. Henderson, N.C. Slowey, U–Th dating of marine isotope stage 7 in Bahamas slope sediments, Earth and Planetary Science Letters 196 (2002) 1–13.

[8] C.D. Gallup, R.L. Edwards, R.G. Johnson, The timing of high sea levels over the past 200,000 years, Science 263 (1994) 796–800.

[9] J. Lundberg, D.C. Ford, Late Pleistocene sea level change in the Bahamas from mass spectrometric U-series dating of submerged speleothem, Quaternary Science Reviews 13 (1994) 1–14.

[10] W.G. Thompson, S.L. Goldstein, Open-system coral ages reveal persistent suborbital sea-level cycles, Science 308 (2005) 401–404.

[11] N.J. Shackleton, M.F. Sánchez Goñi, D. Pailler, Y. Lancelot, Marine isotope substage 5e and the Eemian Interglacial, Global and Planetary Change 36 (2003) 151–155.

[12] C. Spötl, A. Mangini, S.J. Burns, N. Frank, N. Pavuza, Speleothems from the high-Alpine Spannagel Cave, Zillertal Alps (Austria), in: I.D. Sasowsky, J. Mylroie (Eds.), Studies of Cave Sediments: Physical and Chemical Records of Paleoclimate, Kluwer, Dortrecht, 2004, pp. 243–256.

[13] T.C. Atkinson, Growth mechanisms of speleothems in Castleguard Cave, Columbia Icefields, Alberta, Canada, Arctic and Alpine Research 15 (4) (1983) 523–536.

[14] S.E. Lauritzen, Marble stripe karst of the Scandinavian Caledonides: an end-member in the contact karst spectrum, Acta Carsologica 30 (2001) 47–79.

[15] N. Frank, M. Braum, U. Hambach, A. Mangini, G. Wagner, Warm period growth of travertine during the Last Interglaciation in southern Germany, Quaternary Research 54 (2000) 38–48.

[16] H. Cheng, R.L. Edwards, J. Hoff, C.D. Gallup, D.A. Richards, Y. Asmeron, The half-lives of uranium-234 and thorium-230, Chemical Geology 169 (2000) 17–33.

[17] C. Spötl, A. Mangini, N. Frank, R. Eichstädter, S.J. Burns, Start of the Last Interglacial period at 135 ka: evidence from a high Alpine speleothem, Geology 30 (9) (2002) 815–818.
[18] S. Holzkämper, A. Mangini, C. Spötl, M. Mudelsee, Timing and progression of the Last Interglacial derived from a high alpine stalagmite, Geophysical Research Letters 31 (7) (2004) L07201, doi:10.1029/2003GL019112.
[19] C. Spötl, T. Vennemann, Continuous-flow IRMS analysis of carbonate minerals, Rapid Communications in Mass Spectrometry 17 (2003) 1004–1006.
[20] H.K. Wedepohl, The composition of the continental crust, Geochimica et Cosmochimica Acta 59 (7) (1995) 1217–1232.
[21] G.J. Kukla, J.-L. Beaulieu, H. Svobodova, V. Andrieu-Ponel, N. Thouveny, H. Stockhausen, Tentative correlation of pollen records of the Last Interglacial at Grande Pile and Ribains with marine isotope stages, Quaternary Research 58 (2002) 32–35.
[22] C. Spötl, S. Holzkämper, A. Mangini. The Last and the Penultimate Interglacial as recorded by speleothems from a climatically sensitive high-elevation cave site in the Alps, The climate of past interglacials, in: F. Sirocko, T. Litt, M. Claussen and M.F. Sánchez Goñi, (Eds.), Developments in Quaternary Science Series, Elsevier, submitted for publication.
[23] C. Spötl, A. Mangini, Chronology and paleoenvironment of marine isotope stage 3 interstadials from two high-elevation speleothems, Austrian Alps, Quaternary Science Reviews, submitted for publication.
[24] C. Spötl, A. Mangini, Stalagmite from the Austrian Alps reveals Dansgaard–Oeschger events during isotope stage 3: implications for the absolute chronology of Greenland ice cores, Earth and Planetary Science Letters 203 (2002) 507–518.
[25] I.J. Winograd, T.B. Coplen, J.M. Landwehr, A.C. Riggs, K.R. Ludwig, B.J. Szabo, P.T. Kolesar, K.M. Revesz, Continuous 500,000-year climate record from vein calcite in Devils Hole, Nevada, Science 258 (1992) 255–260.
[26] N.J. Shackleton, K.R. Ludwig, K.R. Simmons, I.J. Winograd, B.J. Szabo, J.M. Landwehr, A.C. Riggs, Last interglacial in Devils Hole, Nature 362 (1993) 596.
[27] N.C. Slowey, G.M. Henderson, W.B. Curry, Direct U–Th dating of marine sediments from the two most recent interglacial periods, Nature 383 (1996) 242–244.
[28] T.D. Herbert, J.D. Schuffert, D. Andreasen, L. Heusser, M. Lyle, A. Mix, A.C. Ravelo, L.D. Stott, J.C. Herguera, Collapse of the California Current during glacial maxima linked to climate change on land, Science 293 (2002) 71–76.
[29] A. Baker, P.L. Smart, R.L. Edwards, Mass spectrometric dating of flowstones from stump cross caverns and Lancaster Hole, Yorkshire: palaeoclimatic implications, Journal of Quaternary Science 11 (2) (1996) 107–114.
[30] C.D. Gallup, H. Cheng, F.W. Taylor, R.L. Edwards, Direct determination of the timing of sea level change during Termination II, Science 295 (2002) 310–313.
[31] G.M. Henderson, N.C. Slowey, Evidence from U–Th dating against northern hemisphere forcing of the penultimate deglaciation, Nature 404 (2000) 61–66.
[32] T.M. Esat, M.T. McCulloch, J. Chappell, B. Pillans, A. Omura, Rapid fluctuations in sea level recorded at Huon Peninsula during the penultimate deglaciation, Science 283 (1999) 197–201.
[33] N.J. Shackleton, M. Chapman, M.F. Sánchez Goñi, D. Pailler, Y. Lancelot, The classic marine isotope substage 5e, Quaternary Research 58 (2002) 14–16.
[34] K. Lambeck, J. Chappell, Sea level change through the last glacial cycle, Science 292 (5517) (2001) 679–686.
[35] E.S. Kandiano, H.A. Bauch, A. Müller, Sea surface temperature variability in the North Atlantic during the last two glacial–interglacial cycles: comparison of faunal, oxygen isotopic, and Mg/Ca-derived records, Palaeogeography, Palaeoclimatology, Palaeoecology 204 (2004) 145–164.
[36] X. Wang, A.S. Auler, R.L. Edwards, H. Cheng, P.S. Cristalli, P.L. Smart, D.A. Richards, C.-C. Shen, Wet periods in northeastern Brazil over the past 210 kyr linked to distant climate anomalies, Nature 432 (2004) 740–743.
[37] S.J. Burns, D. Fleitmann, A. Matter, U. Neff, A. Mangini, Speleothem evidence from Oman for continental pluvial events during interglacial periods, Geology 29 (7) (2001) 623–626.
[38] K.B. Cutler, R.L. Edwards, F.W. Taylor, H. Cheng, J. Adkins, C.D. Gallup, P.M. Cutler, G.S. Burr, A.L. Bloom, Rapid sea-level fall and deep-ocean temperature change since the Last Interglacial period, Earth and Planetary Science Letters 206 (2003) 253–271.
[39] M.F. Sánchez Goñi, M.F. Loutre, M. Crucifix, O. Peyron, L. Santos, J. Duprat, B. Malaizé, J.-L. Turon, J.-P. Peypouquet, Increasing vegetation and climate gradient in western Europe over the Last Glacial inception (122–110 ka): data–model comparison, Earth and Planetary Science Letters 231 (2005) 111–130.
[40] H. Linge, S.-E. Lauritzen, J. Lundberg, Stable isotope stratigraphy of a late Last Interglacial speleothem from Rana, northern Norway, Quaternary Research 56 (2001) 155–164.
[41] F. Preusser, C. Schlüchter, Dates from an important early Late Pleistocene ice advance in the Aare Valley, Switzerland, Eclogae Geologica Helvetiae 97 (2004) 245–253.
[42] W. Dreybrodt, A possible mechanism for growth of calcite speleothems without participation of biogenic carbon dioxide, Earth and Planetary Science Letters 58 (1982) 293–299.
[43] A. Mangini, C. Spötl, P. Verdes. Reconstruction of temperature in the Central Alps during the past 2,000 years from a $\delta^{18}O$ stalagmite record, Earth and Planetary Science Letters, in press.
[44] I. Friedman, J.R. O'Neil, Compilation of stable isotope fractionation factors of geochemical interest, in: M. Fleischer (Ed.), Data of Geochemistry, U.S. Geol. Survey, 1977, Prof. Paper 440-kk, pp. 1–12.
[45] C.H. Hendy, The isotopic geochemistry of speleothems: I. The calculation of the effects of different modes of formation on the isotopic composition of speleothems and their applicability as palaeoclimatic indicators, Geochimica et Cosmochimica Acta 35 (1971) 801–824.
[46] H.P. Schwarcz, Geochronology and isotopic geochemistry of speleothems, in: P. Fritz, J.C. Fontes (Eds.), Handbook of Environmental Isotope Geochemistry, Elsevier, Amsterdam, 1986, pp. 271–303. 2B.